Optics Letters

Absolute two-photon excitation spectra of red and far-red fluorescent probes

Mary Grace M. Velasco,[1,2,3] Edward S. Allgeyer,[2] Peng Yuan,[4,5] Jaime Grutzendler,[4,5] and Joerg Bewersdorf[1,2,3,*]

[1]Department of Biomedical Engineering, Yale School of Engineering and Applied Science, 55 Prospect St., New Haven, Connecticut 06511, USA
[2]Department of Cell Biology, Yale School of Medicine, 333 Cedar St., New Haven, Connecticut 06511, USA
[3]Integrated Graduate Program in Physical and Engineering Biology, Yale University, New Haven, Connecticut 06511, USA
[4]Department of Neurology, Yale School of Medicine, 300 George St., New Haven, Connecticut 06510, USA
[5]Department of Neurobiology, Yale School of Medicine, 333 Cedar St., New Haven, Connecticut 06510, USA
*Corresponding author: joerg.bewersdorf@yale.edu

Received 14 July 2015; revised 16 September 2015; accepted 27 September 2015; posted 28 September 2015 (Doc. ID 245756); published 21 October 2015

Efficient use of two-photon excitation (TPE) microscopy requires knowledge of the absolute TPE action cross sections (ATACSs) of fluorescent probes. However, these values are not available for recently developed dyes, which exhibit superior properties in many modern microscopy applications. We report ATACSs of five red to far-red organic dyes, ATTO 647N, STAR 635P, silicon rhodamine, ATTO 594, and ATTO 590. The dyes were found to have large ATACSs (>100 GM) at their respective wavelength peaks, thus supporting their use as bright fluorescent markers in TPE microscopy.

OCIS codes: (180.2520) Fluorescence microscopy; (190.4180) Multiphoton processes; (190.1900) Diagnostic applications of nonlinear optics.

http://dx.doi.org/10.1364/OL.40.004915

Two-photon excitation (TPE) fluorescence microscopy [1,2] is a powerful technique that relies on two-photon absorption (TPA) [3]. It is especially useful for imaging in optically heterogeneous samples due to the use of near-infrared excitation wavelengths that are less susceptible to scattering. Effective TPE microscopy requires fluorescent labels that are easily excitable via TPA. Unfortunately, the TPA properties of a given probe cannot be predicted from its single-photon excitation (SPE) spectrum and therefore require independent quantification. Since the 1990s, the absolute TPE action cross sections (ATACSs) of a wide range of organic dyes and fluorescent proteins have been measured (see, for example, [4–8]) and the data have become an essential reference for the successful application of TPE microscopy. The recent introduction of highly photostable dyes in the red and far-red emission range, such as ATTO 647N, STAR 635P, silicon rhodamine (SiR) [9], ATTO 594, and ATTO 590, offers new opportunities for TPE microscopy. For example, SiR and ATTO 590 are membrane-permeable fluorophores that can be coupled to genetically encoded protein tags for *in vivo* labeling [10]. Also, the five dyes listed above are well suited for stimulated emission depletion (STED) nanoscopy [11], an imaging technique that allows for subdiffraction-limit resolution, due to their compatibility with the popular STED depletion wavelength of 775 nm [10]. These dyes have already been successfully used with SPE-STED nanoscopy [12]. However, because their TPA characteristics have not yet been quantified, they have been of limited use in TPE-STED nanoscopy [13] and TPE microscopy in general.

In this Letter, we report the wavelength-dependent ATACSs of ATTO 647N, STAR 635P, SiR, ATTO 594, and ATTO 590, and we confirm, by imaging immunolabelled COS7 cells, that the dyes are suitable fluorescent labels for TPE microscopy.

A simple optical setup was used for all spectroscopy experiments. TPE was generated using <100 fs pulses from a mode-locked titanium:sapphire (Ti:S) laser, tunable between 690 and 1040 nm (MaiTai HP, Spectra-Physics). The light was passed through a half-wave plate (AQWP05M-980, Thorlabs) and a polarizing beam-splitter cube (PBS252, Thorlabs) to adjust the laser intensity and then through a long-pass filter (BLP01-635R, Semrock) to eliminate any shorter wavelength contributions. The beam was expanded to overfill the back aperture of a 10×, 0.3 NA objective lens (UPlanFl, Olympus), which focused the light into a concavity slide filled with the dye solution. A power meter (PM30 and S130A, Thorlabs) positioned behind the sample monitored the excitation power, which did not exceed 5 mW for all experiments to avoid saturation of the dye. The excited fluorescence was collected by the same objective lens, separated from the excitation beam path by a dichroic beam splitter (T695LPXR, Chroma) and passed through either of two filter combinations: (1) 6 mm of BG40 glass (FGB37, Thorlabs) or (2) two bandpass filters (FF01-630/69 and FF01-630/92; Semrock) separated by 6 mm of KG5 glass (FGS600, Thorlabs). The fluorescence was then focused through a 100 μm pinhole using a 500 mm focal length

tube lens before being detected by a large-area photon multiplier tube (PMT; H10682-01, Hamamatsu Photonics). The PMT counts were recorded using a DAQ board (PCIe-7852R, National Instruments) controlled via LabView.

Initial fluorescence measurements indicated that, at wavelengths <750 nm, the dye emission exhibited a large component that depended linearly on the excitation power. The effect was most prevalent for ATTO 647N, STAR 635P, and SiR. We suspect that this signal was generated by SPE, as the tail of the SPE spectra of these dyes overlaps with the wavelength range of the Ti:S laser. Because this linear signal was much greater than any detected nonlinear signal, we concluded that wavelengths <750 nm would not be suitable for TPE of these dyes, and the wavelengths were excluded from our spectrum plots. Moreover, to eliminate non-TPE generated signals from the measured fluorescence count rates, the fluorescence signal versus excitation power was fit with a second-order polynomial at each wavelength. The linear and constant components of the fit were then subtracted from the total signal recorded to isolate the fluorescence excited via TPA alone. Note that, for all wavelengths tested, the ratio of the TPE to background signal levels was greater than one, indicating that TPE was the predominant source of fluorescence.

The two-photon fluorescence spectrum was then converted to an ATACS spectrum following an approach published previously by Xu and co-workers [4,8]. The following equation was applied at all measured wavelengths:

$$\sigma_{\mathrm{TPE,new}} = \frac{\langle F(t)\rangle_{\mathrm{new}}}{\langle F(t)\rangle_{\mathrm{ref}}} \cdot \frac{\phi_{\mathrm{ref}}}{\phi_{\mathrm{new}}} \cdot \frac{C_{\mathrm{ref}}}{C_{\mathrm{new}}} \cdot \frac{\langle P_{\mathrm{ref}}(t)\rangle^2}{\langle P_{\mathrm{new}}(t)\rangle^2} \cdot \frac{n_{\mathrm{ref}}}{n_{\mathrm{new}}} \cdot \sigma_{\mathrm{TPE,ref}}. \quad (1)$$

Here, $\langle F(t)\rangle$ is the time-averaged fluorescence signal, measured as discussed above. $\langle P(t)\rangle^2$ is the square of the time-averaged excitation power measured behind the sample throughout the experiment. C and n are the concentration and refractive index of the sampled dye solution, respectively. ϕ is the dye-specific collection efficiency of the detection optics, calculated with respect to the transmission specifications of the dichroic and emission filters, the quantum efficiency of the PMT, and the normalized fluorescence emission spectra of the dye. All emission spectra were measured using a spectrofluorometer (QuantaMaster, Photon Technology International). σ_{TPE} is the ATACS of the dye, where σ_{TPE} is the product of the absorption cross section of the dye, σ_{TPA}, and its quantum yield, η. The subscripts "new" and "ref" correspond to the dye being investigated and a reference dye, respectively. As discussed in [5], the calibration of measured data with respect to the known ATACSs of a reference dye, eliminates the need to quantify the excitation laser parameters that greatly affect TPE efficiency. For all experiments, fluorescein or rhodamine B was used as a calibration standard, and their ATACSs were retrieved from [4].

To prepare samples, the dyes were first dissolved in the appropriate solvents (listed in Table 1). The reference dyes fluorescein and rhodamine B were used in their free, unbound form while a Cyanine 3 (Cy3) derivative containing a free amino group was used to ensure the dye's solubility in water. The latter was used as a positive control for our protocols. All other dyes, except SiR, were utilized as NHS esters or NHS carbonates. Due to the fluorogenic nature of SiR [9], the NHS ester was conjugated to antibodies prior to sample preparation. ATTO 647N streptavidin and ATTO 594 antibodies were also tested to investigate the effect of protein conjugation on the ATACSs of the dyes. Next, solution concentrations were calculated from single photon absorbance measurements and extinction coefficients using Beer's law. Absorbance was measured at the SPE wavelength maximum of each dye using a spectrophotometer (SmartSpec Plus, Bio-Rad), while extinction coefficients were retrieved from the supplier data. Solution concentrations are also listed in Table 1. Finally, approximately 100 μl of each dye solution was pipetted onto a concavity slide, and the well was sealed with Nexterion cleanroom cleaned coverslips (1472306, Applied Microarrays) to minimize any autofluorescent signal from the glass.

To confirm the validity of our setup and protocols, we first generated the ATACS of Cy3, whose TPE spectrum is already well established [5]. This data is presented in Fig. 1, together with the Cy3 spectrum reported in [5]. The spectra are in good agreement, thus confirming the reliability of our procedure.

Figure 2 presents the absolute TPE spectra of the dyes investigated in this Letter. It is interesting to note the significant blueshift of the TPE spectrum wavelength peak from twice the corresponding SPE wavelength peak. For some dyes (e.g., ATTO 594 and ATTO 590), weak peaks occur at ~1000 nm, which coincide with the onset of the SPE excitation spectrum at ~500 nm. The main TPE peak, however, corresponds to a weaker blueshifted peak in the SPE spectrum at ~400 nm, as demonstrated by the dashed curves. This peak represents excitation to an energy level higher than the first excited electronic state [14]. The existence of a peak in the ~800 nm range is an advantageous feature of these dyes, as it renders them excitable by the traditional Ti:S lasers most commonly used in TPE microscopy.

Table 1. Dye Suppliers, Solvents, and Concentrations

	Product Number and Supplier	Solvent	Concentration (μM)
Fluorescein	46955, Sigma Aldrich	Water (pH 13)	14.6
Cy3 amine	110C0, Lumiprobe	Sodium carbonate (pH 9)	65.1
Rhodamine B	83689, Sigma Aldrich	Methanol	14.7
ATTO 647N NHS ester	18373, Sigma Aldrich	Phosphate buffered saline	38.6
ATTO 647N—streptavidin	94149, Sigma Aldrich	Phosphate buffered saline	46.0
ATTO 594 NHS ester	08741, Sigma Aldrich	Phosphate buffered saline	3.25
Anti-Mouse IgG—ATTO 594	76085, Sigma Aldrich	Phosphate buffered saline	5.21
ATTO 590 NHS ester	79636, Sigma Aldrich	Phosphate buffered saline	3.18
STAR 635P NHS carbonate	1-0101-007-6, Abberior	Phosphate buffered saline	25.6
SiR NHS ester	SC003, Spirochrome	Phosphate buffered saline	34.8

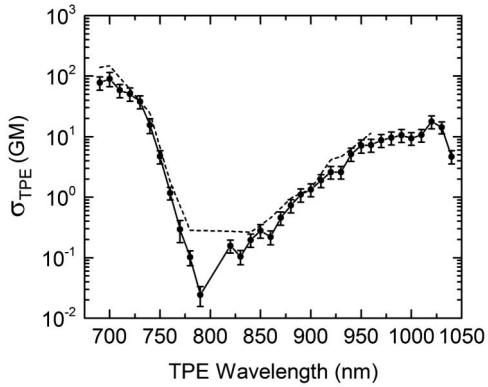

Fig. 1. Measured TPE spectrum of Cy3 amine (solid) and the Cy3 TPE spectrum reported in [5] (dashed). Error bars represent the standard error of the mean, where $n = 3$.

Figures 2(a) and 2(d) compare the absolute TPE spectrum of ATTO 647N streptavidin and ATTO 594 antibodies to that of the corresponding NHS ester. The spectra corresponding to the same dye show identical peaks. However, the dye-labeled proteins show ATACSs that are a factor of ~2–3 lower than those of the NHS ester. This can be attributed to the quenching characteristics of the different groups labeled by the dye, as discussed in [15].

Figure 2(f) presents the dependence of the raw fluorescence signal on excitation power. The wavelengths for optimum TPE were identified from the spectra in Figs. 2(a) and 2(e), and the square law dependence was tested at these wavelengths to confirm TPE. Note that no background correction was performed on these fluorescence measurements. For excitation powers less than 10 mW, the deviation from perfect square dependence on power was well within experimental error for all fluorophores, thus confirming TPE without any significant contributions from linear effects.

To confirm the two-photon excitability of the dyes in a biological sample, fluorescently labeled COS7 cells were prepared using standard immunohistochemistry protocols. The samples were then imaged on a TPE microscope (Prairie Ultima, Prairie Technologies) equipped with a Zeiss 20 × /1.0 NA objective lens. Mitochondria and microtubules were labeled using TOM20 (T5168, Sigma Aldrich) and alpha-tubulin (sc-11415, Santa Cruz) antibodies, respectively. The appropriate excitation wavelengths were identified from the spectra in Figs. 2(a)–2(e): 840 nm for ATTO 647N, 820 nm for STAR 635P, and 800 nm for ATTO 594. The acquired TPE microscopy images (Fig. 3) are bright and show low background. Furthermore, for all six areas imaged, at least 50 single frames could be acquired with negligible (less than 20%) decrease in brightness. This indicates that ATTO647N, STAR635P, and ATTO594 are relatively stable when excited via TPE and confirms that they are suitable dyes for TPE microscopy.

In conclusion, we report the absolute TPE spectra of the red to far-red dyes ATTO 647N, STAR 635P, SiR, ATTO 594, and ATTO 590. The spectrum peaks occur between 800 and 840 nm, and they reveal high ATACS values >100 GM. These values are comparable with the ATACSs of fluorescent proteins [6]. In addition, these dyes offer the advantage of redshifted emission wavelengths that are easily excited using a traditional Ti:S laser. This finding, in combination with the TPE microscopy images acquired in fixed cells, show that these dyes are well suited for TPE microscopy (and likely TPE-STED nanoscopy). With the appropriate labeling protocols, applications can easily be extended to tissue samples and, with the use of the cell permeable dyes SiR and ATTO 590 [10], to *in vivo* applications as well.

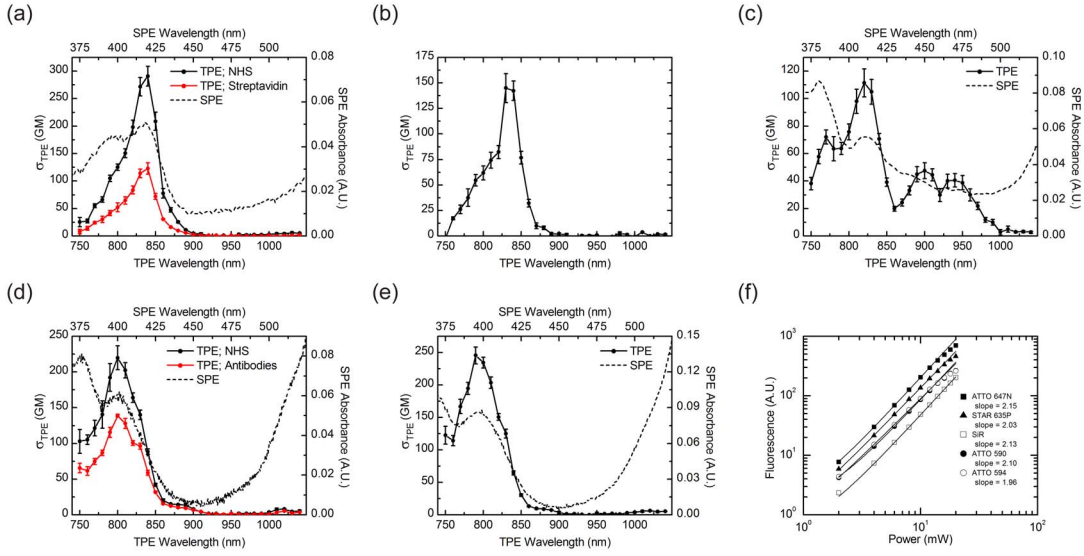

Fig. 2. TPE properties of five STED compatible red to far-red dyes. (a)–(e) Absolute TPE spectra (solid) with corresponding SPE spectra (dashed). SPE spectra were cited from the supplier data. Error bars represent the standard error of the mean, where $n = 3$ or 5. (a) ATTO 647N NHS ester (black) and ATTO 647N streptavidin (red). (b) Silicon Rhodamine (SiR) labeled antibodies. (c) STAR 635P NHS carbonate. (d) ATTO 594 NHS ester (black) and ATTO 594 labeled antibodies (red). (e) ATTO 590 NHS ester. (f) Logarithmic plots of the dependence of TPE generated fluorescence on the incident excitation power. Experiments were performed at the optimum TPE wavelength identified in (a)–(e).

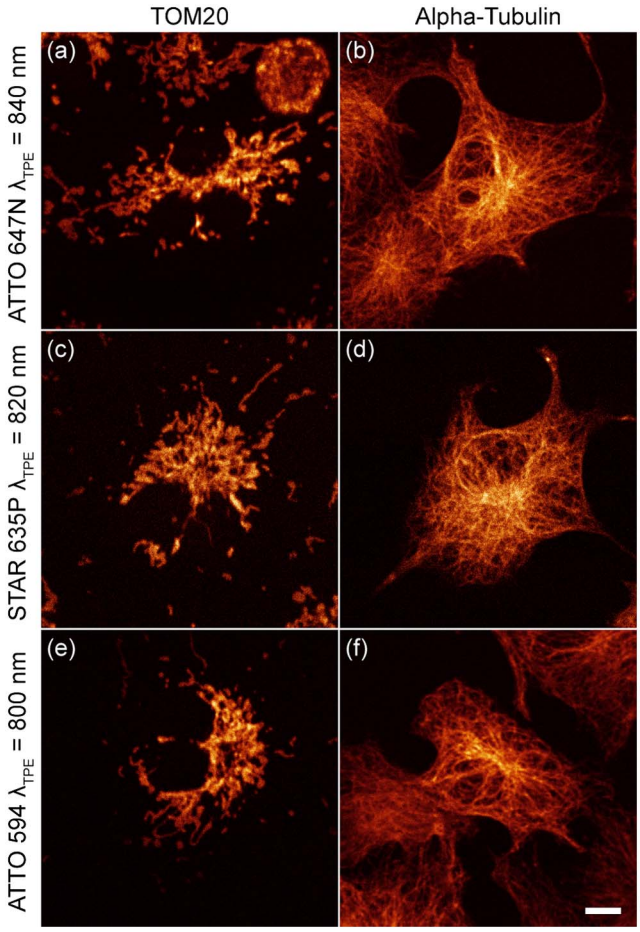

Fig. 3. TPE microscopy images of fluorescently labeled fixed COS7 cells. Mitochondria in (a), (c), and (e) and microtubules in (b), (d), and (f) were labeled using TOM20 and alpha-tubulin antibodies, respectively. Each image is an average of four single frame acquisitions (pixel size: 82 nm, pixel dwell time: 8 μs). λ_{TPE} is the excitation wavelength used. Excitation power, measured at the sample, was 4.5 mW, 5.6 mW, and 2.4 mW for (a), (c), and (e), respectively, and 5.0 mW for (b), (d), and (f). Scale bar is 10 μm.

Funding. G Harold and Leila Y. Mathers Foundation; National Institute of Diabetes and Digestive and Kidney Diseases (NIDDK) (P30-DK45735); National Institute of Neurological Disorders and Stroke (NINDS) (1R01NS089734); Raymond and Beverly Sackler Institute for Biological Physical and Engineering Sciences, Yale University.

Acknowledgment. The authors thank Mark Lessard for sample preparation, Francesca Bottanelli for the supply of dyes, Alexander Thompson for assistance with emission spectrum measurements, and Xiang Hao, Lena Schroeder, and Emil Kromann and Evangelos Gatzogiannis for helpful discussions.

REFERENCES

1. W. Denk, J. H. Strickler, and W. W. Webb, Science **248**, 73 (1990).
2. W. R. Zipfel, R. M. Williams, and W. W. Webb, Nat. Biotechnol. **21**, 1369 (2003).
3. M. Göppert-Mayer, Ann. Phys. **401**, 273 (1931).
4. C. Xu and W. W. Webb, J. Opt. Soc. Am. B **13**, 481 (1996).
5. M. A. Albota, C. Xu, and W. W. Webb, Appl. Opt. **37**, 7352 (1998).
6. M. Drobizhev, N. S. Makarov, S. E. Tillo, T. E. Hughes, and A. Rebane, Nat. Methods **8**, 393 (2011).
7. G. A. Blab, P. H. M. Lommerse, L. Cognet, G. S. Harms, and T. Schmidt, Chem. Phys. Lett. **350**, 71 (2001).
8. C. Xu and W. R. Zipfel, Cold Spring Harb. Protoc. **2015**, 250 (2015).
9. G. Lukinavicius, K. Umezawa, N. Olivier, A. Honigmann, G. Yang, T. Plass, V. Mueller, L. Reymond, I. R. Correa, Jr., Z. G. Luo, C. Schultz, E. A. Lemke, P. Heppenstall, C. Eggeling, S. Manley, and K. Johnsson, Nat. Chem. **5**, 132 (2013).
10. F. Bottanelli, E. B. Kromann, E. S. Allgeyer, R. S. Erdmann, S. W. Baguley, G. Sirinakis, A. Schepartz, D. Baddeley, D. K. Toomre, J. E. Rothman, and J. Bewersdorf, "Live-cell nanoscale imaging of two intracellular targets" (submitted).
11. S. W. Hell and J. Wichmann, Opt. Lett. **19**, 780 (1994).
12. S. W. Hell, Angew. Chem. Int. Ed. **54**, 2 (2015).
13. G. Moneron and S. W. Hell, Opt. Express **17**, 14567 (2009).
14. M. Drobizhev, N. S. Makarov, T. Hughes, and A. Rebane, J. Phys. Chem. B **111**, 14051 (2007).
15. H. Chen, S. S. Ahsan, M. E. B. Santiago-Berrios, H. D. Abruña, and W. W. Webb, J. Am. Chem. Soc. **132**, 7244 (2010).